2376 J. Med. Chem. 2010, 53, 2376–2382
DOI: 10.1021/jm9011615

Journal of Medicinal Chemistry Article

Fluorescent Epigenetic Small Molecule Induces Expression of the Tumor Suppressor Ras-Association Domain Family 1A and Inhibits Human Prostate Xenograft

Kathryn D. Sheikh,[†] Partha P. Banerjee,[‡] Shankar Jagadeesh,[‡] Scott C. Grindrod,[†] Li Zhang,[†] Mikell Paige,[†] and Milton L. Brown*,[†]

[†]*Drug Discovery Program, Department of Oncology, Georgetown University, 3970 Reservoir Road NW, Washington, D.C. 20057, and* [‡]*Department of Biochemistry and Molecular and Cellular Biology, Georgetown University Medical Center, 3900 Reservoir Road NW, Washington, D.C. 20057*

Received August 4, 2009

Epigenetic silencing of Ras-association domain family 1A (RASSF1A) protein in cancer cells results in a disruption of cell cycle control, genetic instability, enhanced cell motility, and apoptotic resistance. Ectopic expression of RASSF1A reverses this tumorigenic phenotype. Thus, small molecules with the ability to restore RASSF1A expression may represent a new class of therapeutic agents. Recently, we designed and synthesized a fluorescent carbazole analogue of mahanine (alkaloid from *Murraya koenigii*) that restored RASSF1A mRNA expression. Our fluorescent lead compound up-regulated RASSF1A *in vitro*, potently inhibited human prostate cancer cell proliferation, and fluoresced at a visible wavelength, allowing for the observation of intracellular distribution. The small molecule lead was not acutely toxic up to 550 mg/kg, and dosing at 10 mg/kg reduced human xenograft tumor volume by about 40%.

Introduction

Ras-association domain family 1A (RASSF1A[a]) is a frequently inactivated protein in human cancer.[1] One of the most commonly found aberrations in human tumors is promoter methylation of the *RASSF1A* gene, which results in a loss of RASSF1A protein expression.[2] This loss of protein expression has been linked to disruptions in cell cycle control, genetic instability, enhanced cell motility, and apoptotic resistance in cancer cells, thus implicating RASSF1A as a tumor suppressor protein.[1,2]

Located on chromosome 3p21.3, the *RASSF1* gene locus codes for seven different transcripts, with RASSF1A expressed as one of two major isoforms in normal cells. The family of proteins share a conserved motif, the RalGDS/AF6 Ras association (RA) domain, as well as a C-terminal SARAH protein−protein interaction motif. Because RASSF1A appears to lack any enzymatic activity, it has been recently hypothesized that it may serve as a scaffolding protein, binding pertinent effector proteins such as K-Ras, proapoptotic kinase MST1 and modulator of apoptosis 1 (MOAPl) through its RA and SARAH domains.[1] Ectopic expression of RASSF1A in cancer cell lines causes G_1/S arrest by reducing cyclin D1 accumulation, promotes genetic stability by stabilizing polymerized microtubules, restores cell−cell adhesion, inhibits motility, and induces apoptosis by mediating the proapoptotic effects of K-Ras.[1,3−6] Because of this reversal of tumorigenic phenotype, small molecules with the ability to restore RASSF1A expression have immense potential in the treatment of tumors.

In prostate cancer, loss of function of classic tumor suppressor genes such as RB1 is not frequently found; however, the *RASSF1A* promoter region is methylated in 71% of primary prostate tumors. When considering only more aggressive prostate tumors (Gleason score of 7−10), the incidence of *RASSF1A* methylation increases to nearly 85%.[7,8] In contrast, *RASSF1A* promoter methylation is not found in normal primary prostate epithelial and stromal cells.[9]

The natural product mahanine (Chart 1) is a potent inhibitor of androgen dependent (LNCaP) and androgen independent (PC-3) human prostate cancer cell proliferation. An increase in RASSF1A expression was previously observed in mahanine-treated LNCaP and PC-3 cells, as well as a decrease in the level of cyclin D1 expression.[10] This is consistent with earlier findings that increased RASSF1A expression down-regulates cyclin D1, resulting in inhibited cell growth.[5] The antiproliferative activity of mahanine was associated with its inhibition of DNA methyltransferase (DNMT) activity in LNCaP and PC-3 cells. Presumably, inhibition of DNMT activity by mahanine prevents the hypermethylation and subsequent silencing of the *RASSF1A* gene in these cell lines. Such epigenetic regulation of *RASSF1A* and other hypermethylated genes has been observed in a variety of human cell lines, including prostate cancer.[7,11,12]

In an effort to discover a novel and more potent small molecule with a mechanistic profile similar to that of mahanine, a variety of synthetic analogues were designed and synthesized, including derivatives containing a fluorescent moiety. These mahanine analogues were evaluated for their effects on PC-3 cell proliferation, RASSF1A expression, cyclin D1 expression, and DNMT activity, and the lead

*To whom correspondence should be addressed. Phone: (202) 687-8603. Fax: (202) 687-5659. E-mail: mb544@georgetown.edu.

[a] Abbreviations: AOT, acute oral toxicity; dansyl, 5-(dimethylamino)naphthalene-1-sulfonyl; DCB, dichlorobenzene; DCM, dichloromethane; DNMT, DNA methyltransferase; GI_{50}, concentration of drug needed to inhibit cell growth by 50%; PEG, polyethylene glycol; RASSF1A, Ras-association domain family 1A; RT-PCR, reverse transcription polymerase chain reaction; TEA, triethylamine.

 Published on Web 02/25/2010

Chart 1. Structure of Mahanine and Template for Structural Modifications

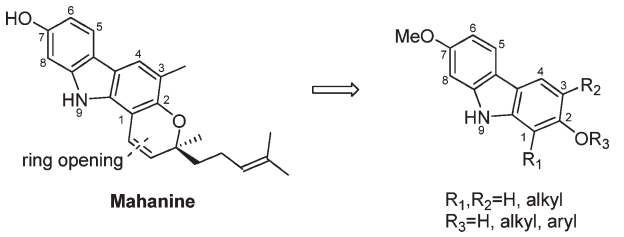

compound was evaluated in an in vivo human prostate tumor model.

Results and Discussion

Chemistry. Modifications of the carbazole backbone that result from a ring-opening strategy of the chromene ring of mahanine were selected as the primary synthetic focus (Chart 1). The alkyl and aryl substituents detailed below (R_1 = H, Me; R_2 = H, Bn, dansyl) were chosen to roughly probe the three-dimensional space around the eastern half of the carbazole backbone. The formation of the carbazole moiety can be envisioned through the cyclization of a biaryl system. To create the initial biaryl moiety (**4**), a direct cross-coupling of aryl halides **2** and **3** using a substrate-specific reaction was found to be applicable to our system (Scheme 1).[13] Contrary to what was expected from reported observations,[13] we found the nitro-substituted aryl bromide **3** to be far more reactive than the aryl iodide **2**. Homocoupling of **3** was observed to some extent under all of our conditions, even when used as the limiting reagent, while homocoupling of **2** only occurred when reactions were allowed to run for several days. No reactions occurred at temperatures under 90 °C, while temperatures over 130 °C resulted in little cross-coupling, yielding only the homocoupled products.

The biaryl **4** was cyclized to give the two possible regioisomers, **5** and **6**, which were separable by column chromatography (Scheme 1).[14] The structural assignment of the two isomers was based on the ^{1}H NMR coupling patterns of the aryl protons. The ^{1}H NMR spectrum of compound **5** showed two doublets (δ 6.91 and 7.73, J = 8.4 Hz) corresponding to the protons on carbons 3 and 4, respectively, whereas the ^{1}H NMR spectrum of compound **6** showed two singlets (δ 6.89 and 7.72) corresponding to the protons on carbons 1 and 4, respectively. Compounds **5** and **6** were produced in an approximately 1:1 ratio of regioisomers as determined by the mass of each isolated isomer after column chromatography, regardless of the reaction conditions. Varying the solvent (1,2- or 1,3-dichlorobenzene) as well as the equivalents of triphenylphosphine resulted in only nominal changes in the ratio of regioisomers. A palladium-on-carbon mediated deprotection of the benzyl groups of **5** and **6** provided the alcohols **7** and **8**, respectively, which were reacted with dansyl chloride to give the fluorescent analogues **9** and **10**, respectively.

Mahanine Analogues Inhibit Growth of Human Prostate Cancer Cells without Cytotoxicity. Compounds **5**−**10** were screened for their effects on growth inhibition of PC-3 human prostate cancer cells using previously reported methods (Table 1).[15] Compound **5** and the related analogue **9** showed markedly improved inhibition compared to their counterparts **6** and **10**, respectively, though the two sets of compounds differed only in the position of the methyl group (i.e., 1-position versus 3-position). This was unexpected, since the methyl group of mahanine is in the 3-position.

Compound **8**, however with a methyl group in the 3-position but a deprotected hydroxyl group in the 2-position, exhibited a GI_{50} value near those of compounds with a 1-position methyl (i.e., **7** and **9**). It is possible that the benefit of the free hydroxyl was due to the reduction of steric bulk at the 2-position or the formation of a hydrogen bond. Nevertheless, it is obvious when comparing the more potent analogues **5**, **7**, and **9** that increasing bulk at the 2-position greatly enhances potency when the methyl is in the 1-position.

Overall, only **9** provided slightly greater antiproliferative effects on human prostate cancer cells compared to mahanine. Additionally, mahanine was observed to be cytotoxic at 24 h at doses greater than 5 μM, while **9** proved to be largely cytostatic at concentrations up to 30 μM (data not shown). This observation was substantiated by testing performed at the National Cancer Institute (NCI) with compound **9** against 59 cell lines, where concentrations of **9** up to 100 μM resulted in no negative growth in 55 of the cell lines (93%) and no instances of total cell kill in any of the cell lines (p S2 of Supporting Information).

New Synthetic Analogues Induced a Decrease in DNA Synthesis. To assess the levels of DNA synthesis within prostate cancer cells treated with compounds **5**−**10**, cultured cells were treated for 24 h with either mahanine or compounds **5**−**10** and then treated with 5-bromo-2-deoxyuridine (BrdU) (Figure 1). Only three of the synthetic compounds (**5**, **8**, and **9**) paralleled mahanine in causing a decrease in DNA synthesis. Because DNA synthesis is associated with cell proliferation, it is not surprising that cells treated with **5** and **9** exhibited lower BrdU uptake than those treated with **6** or **10**, given the respective GI_{50} values of the compounds.

Up-Regulation of RASSF1A and Down-Regulation of Cyclin D1 Was Observed in Cells treated with Mahanine Analogues. It has been reported that mRNA levels of RASSF1A correlate to its protein expression levels.[4] Therefore, to investigate the effects of the synthetic compounds on RASSF1A expression and cyclin D1 expression, levels of the respective mRNAs in treated prostate cancer cells and untreated control cells were determined by RT-PCR (Figure 2). Like mahanine, compounds **5** and **9** up-regulated RASSF1A, with **5** eliciting a response on par with mahanine and **9** increasing RASSF1A levels about 50% more than that of mahanine treatment (Figure 3, gray bars). This occurred with a corresponding decrease in cyclin D1 levels. A similar profile was also observed in **7** and **8** but to a lesser extent. Because overexpression of cyclin D1 is generally associated with tumorigenicity and proliferation in a variety of tumors, including prostate cancers, this down-regulation may have a broader clinical significance.[16,17] Compounds **6** and **10** show no change in expression levels from that of untreated control.

New Synthetic Compounds Inhibited DNA Methyltransferase Activity. By use of a DNMT assay kit from Epigentek, the levels of DNMT activity in treated versus untreated prostate cancer cells were measured. Significant inhibition of DNMT activity was observed with mahanine and compounds **5** and **9**, with **9** causing the most potent inhibition (Figure 3, black bars). A slight decrease in DNMT activity was also associated with compounds **7** and **8**. These reduced DNMT activities correlate with the pattern of RASSF1A induction described above (Figure 3, gray bars). We propose that the inhibition of DNMT prevents hypermethylation of the RASSF1A promoter region and consequently restores

Scheme 1[a]

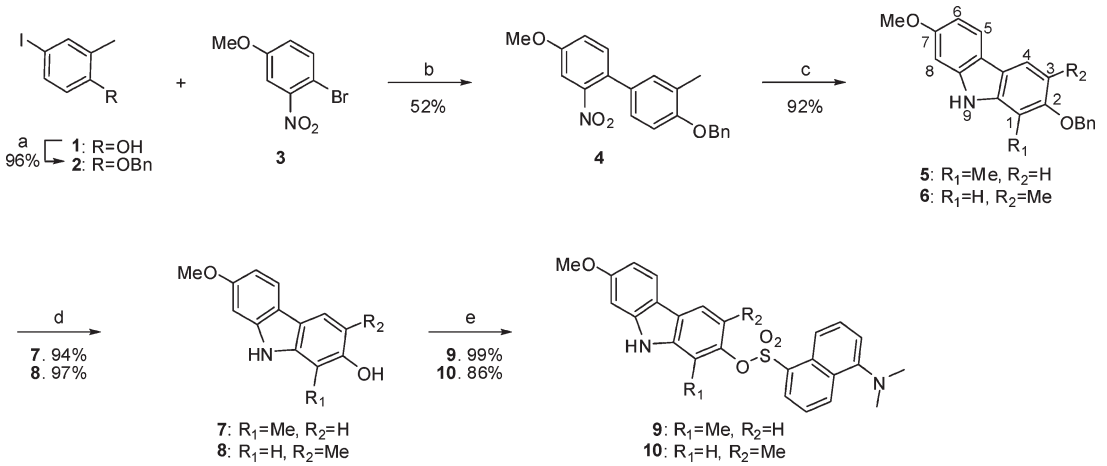

[a] (a) Benzyl bromide, K_2CO_3, MeCN, 50 °C; (b) $Pd(OAc)_2$, K_2CO_3, PEG, 120 °C; (c) PPh_3, 1,3-dichlorobenzene, reflux; (d) Pd/C (5 wt %), ammonium formate, MeOH; (e) dansyl chloride, TEA, DCM.

Table 1. GI_{50} Values for Mahanine and Analogues **5**−**10** in Human Prostate Cancer Cells[a]

compd	GI_{50} (μM)
mahanine	2.5 ± 0.18
5	17.6 ± 2.7
6	48.9 ± 1.1
7	18.7 ± 1.8
8	15.3 ± 2.8
9	1.5 ± 0.11
10	22.9 ± 4.5

[a] Concentrations required for 50% growth inhibition in PC-3 cells. Cells were plated in triplicate wells and exposed to various concentrations (0, 1, 5, 15, 30, 60 μM) of each compound. After 24 h of treatment, viable cells (as assessed by trypan blue dye exclusion assay) were counted using a hemocytometer. Values are the mean ± SEM of three independent observations.

RASSF1A protein, ultimately decreasing cyclin D1 levels and causing the observed human prostate cancer cell growth inhibition.

Fluorescent Analogue 9 Confirmed Intracellular Delivery and Revealed Cellular Localization. The dansyl moiety present in compound **9** allows it to visibly fluoresce at 552 nm when excited at 370 nm (Figure 4A). After treatment of PC-3 cells with **9**, a multiphoton laser was used to excite the compound, and its emission from within the cells was observed by confocal microscopy (Figure 4B−D). With propidium iodide (blue) staining the nuclei of the cells, it was apparent that **9** (green) was present within the cytoplasm of the cells but not in the nuclei (Figure 4B,C). To test the hypothesis that **9** interaction with DNMT is a crucial factor in the ultimate up-regulation of RASSF1A, the cell samples were stained with antibodies for the DNMT isoforms known to shuttle between the nucleus and the cytoplasm, i.e., DNMT3a and DNMT3b.[18,19] Interestingly, while DNMT3b (red) was present in both the cytoplasm and nuclei of the control cells (Figure 4D), after 1 h there was a population of treated cells that had DNMT3b only in the cytoplasm (Figure 4B, arrows). By 6 h this effect was very pronounced, with the majority of treated cells having DNMT3b only in the cytoplasm (Figure 4C). No such corresponding effect was seen with DNMT3a (data not shown), suggesting that this effect was not global inhibition of nuclear access. This cytoplasmic sequestering could be indicative of a mode of action for **9**, but further studies are required.

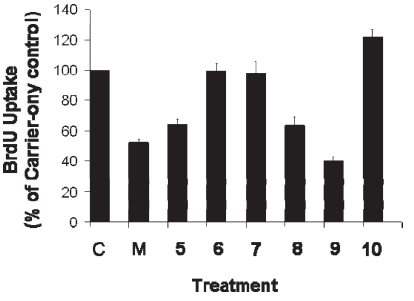

Figure 1. Mahanine analogues decrease DNA synthesis in PC-3 cells. PC-3 cells were plated in 96-well plates and treated with 5 μM mahanine (M), synthetic analogue (number), or DMSO (C). After 24 h, the cells were assayed for BrdU labeling using the cell proliferation ELISA BrdU kit from Roche. Background BrdU incorporation levels (absent anti-BrdU-peroxidase solution) were subtracted, and values were normalized to those of control untreated cells. Values are presented as the mean ± SEM.

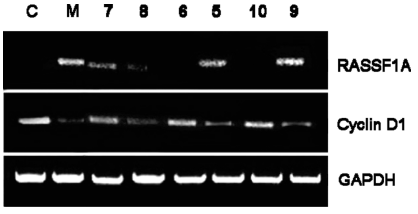

Figure 2. Mahanine analogues induce RASSF1A expression and down-regulate cyclin D1. PC-3 cells were treated 72 h with either 5 μM compound (mahanine (M), **9**) or 15 μM compound (**5**, **6**, **7**, **8**, **10**, DMSO (C)) before RNA extraction and RT-PCR amplification.

Preliminary in Vivo Studies Indicated a Large Therapeutic Index and Significant Volume Reduction of Human Prostate Xenograft Tumors in Mice Treated with the Lead Compound 9. By use of the acute oral toxicity (AOT) up-and-down procedure, no toxicity was observed for compound **9** in wild-type Balb/c mice dosed up to 550 mg/kg.[20] This provided an estimated therapeutic index of > 55 at a starting efficacy dose of 10 mg/kg. Athymic Balb/c nude mice with human prostate tumor xenografts were dosed via intraperitoneal injection with 10 mg/kg **9** once a day every other day for 28 days. Control mice were dosed with vehicle alone. Compound **9** reduced tumor volume by about 40% compared to control

over 28 days (Figure 5A), with statistically significant T/C ratios[21] for all but two time points (Figure 5B). Although dose-escalating studies have yet to be performed to find the optimum dose and schedule, these results demonstrate the potential use of this compound for reducing human prostate tumor volume.

Conclusions

Over the past 5 years, epigenetic regulation in cancer has quickly risen to the forefront of cancer research.[22,23] By

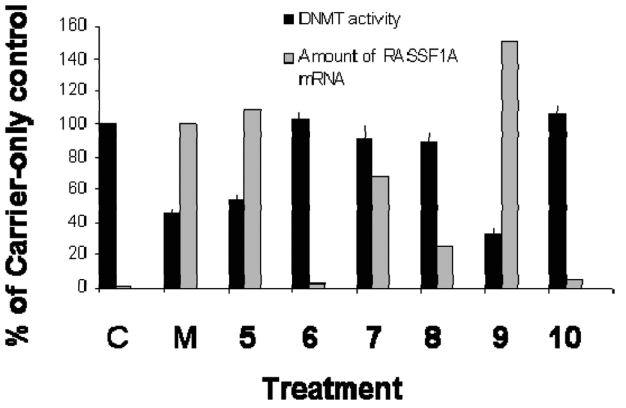

Figure 3. Mahanine analogues that up-regulate RASSF1A also inhibit DNA methyltransferase activity. Black bars: PC-3 cells were treated 72 h with either 2 μM compound (mahanine, **9**) or 15 μM compound (**5**, **6**, **7**, **8**, **10**) and then assayed for DNMT activity using the DNMT activity kit from Epigentek. Data are the mean of three independent experiments ± SEM. Gray bars: Densitometry from RT-PCR blot is shown where the amount of RASSF1A mRNA re-expressed by mahanine treatment is normalized to 100%.

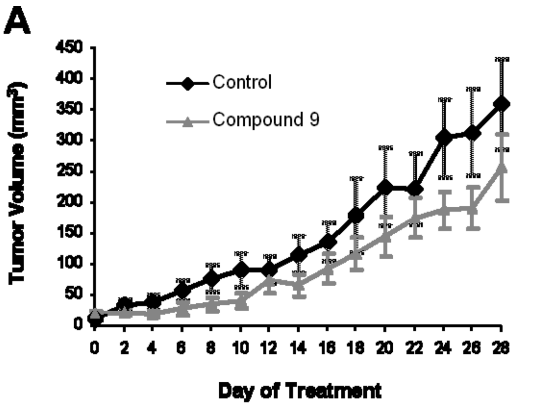

B

Day	0	2	4	6	8	10	12
T/C	0.41	0.42	0.42	0.37	0.39	0.68	0.48
14	16	18	20	22	24	26	28
0.56	0.52	0.52	0.63	0.48	0.47	0.50	0.58

Figure 5. Treatment with compound **9** reduces the volume of human prostate xenograft tumors. (A) Male athymic Balb/c nude mice were injected with PC-3 cells and the resulting tumors allowed to grow for a week before dosing ip once a day every other day with 10 mg/kg compound **9** or DMSO control in 1:1 PEG/PBS. Data are presented as the mean ± SEM (n = 4). (B) T/C is defined as the relative sizes of treated (t) and control (c) tumors and is calculated using T/C = (t RTV)/(c RTV), where RTV = V_t/V_0. V_0 represents the volume at time zero, and V_t is the volume at the given time point. $T/C > 0.60$ is defined as null, and $T/C < 0.60$ is defined as effective (statistically significant).

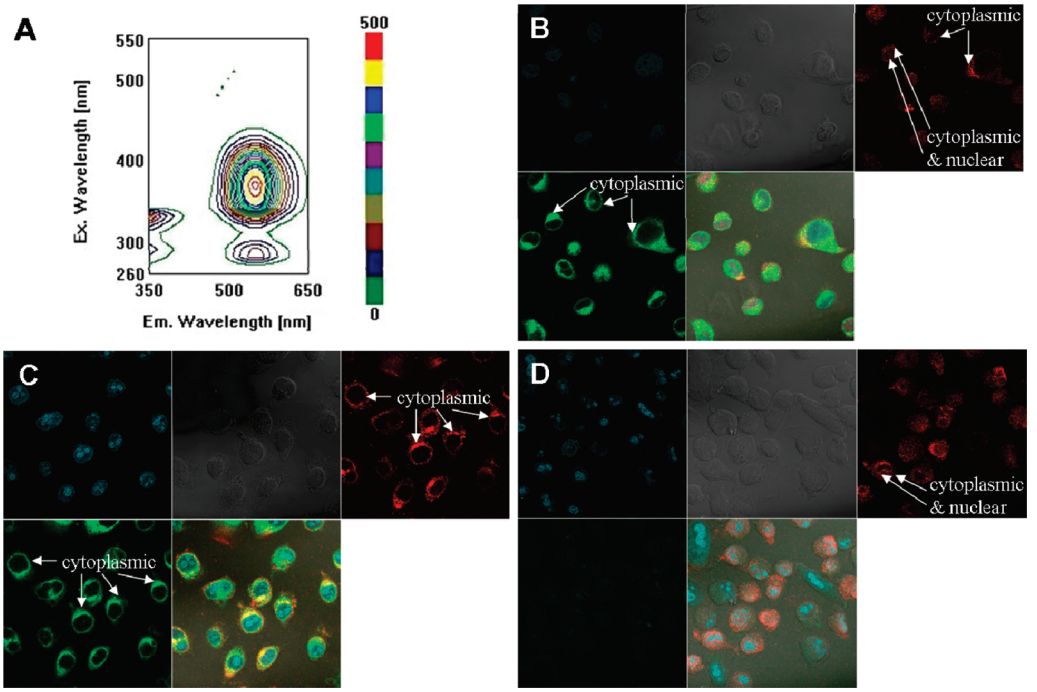

Figure 4. Fluorescent analogue **9** is seen exclusively in the cytoplasm of PC-3 cells and appears to sequester DNMT3b in the cytoplasm. (A) Fluorescent spectrum of **9** is shown. (B) PC-3 cells were treated with a 5 μM solution of **9** for 1 h before being fixed and stained with propidium iodide and DNMT3b antibody. (C) Cells were treated with a 5 μM solution of **9** for 6 h before fixation. (D) Cells were treated with a 5 μM solution of DMSO for 6 h before fixation. The frames in each set of images are as follows, from left to right and from top to bottom: propidium iodide (blue); clear field; DNA methyltransferase 3b (DNMT3b) (red); compound **9** (green) or vehicle; and merged. Compound **9** was excited at 725 nm with a multiphoton laser and imaged with a 500−550 nm filter. Arrows indicate the subcellular localization of DNMT3b.

synthesizing and testing analogues of the natural product mahanine, we have found a compound, **9**, that possesses several advantages as a possible epigenetic prostate cancer therapeutic. Compound **9** inhibited human prostate cancer cell proliferation at 1.5 μM while avoiding cytotoxic effects seen with mahanine treatment, and it fluoresced, providing visual evidence of the compound entering human prostate cancer cells. Like mahanine, compound **9** up-regulated tumor suppressor protein RASSF1A and down-regulated cyclin D1. It also inhibited DNMT activity, proposed to be the event leading to the restoration of RASSF1A expression. Indeed, depletion of one of the three active DNMT isoforms, DNMT3b, has been shown to cause potent antiproliferation and restoration of RASSF1A expression in cancer cell lines.[11] Preliminary data suggest that **9** may have some effect on DNMT3b, though further investigation remains to determine the precise mechanism of action. Regardless of DNMT isoform specificity, we predict **9** will possess an improved therapeutic index compared to current DNMT inhibitors, since it is the irreversible DNMT-binding action of current nucleoside DNMT inhibitors that is associated with significant cytotoxicity.[22] Preliminary in vivo studies of the RASSF1A up-regulator **9** lend credence to this prediction and justify studying compound **9** in more advanced preclinical models of prostate cancer.

Experimental Section

All reagents and solvents were purchased from commercial suppliers and used as received unless noted otherwise. Flash column chromatography separations were done on a Biotage SP1 system monitoring at 254 and 310 nm. NMR spectra were recorded on a Varian 400 spectrometer at 22.5 °C, operating at 400 MHz for ^{1}H and 100 MHz for ^{13}C NMR. The chemical shifts are expressed in ppm downfield from TMS as an internal standard ($CDCl_3$ or DMSO-d_6 solution). Melting points were determined in open capillary tubes on an Electrothermal melting point apparatus and are uncorrected. Compound purity of at least 95% was established by combustion analysis and confirmed by HPLC and HRMS when deemed appropriate. Elemental analyses were performed by Atlantic Microlab, Inc. (Norcross, GA). HPLC traces were recorded with a Shimadzu LC20-series LCMS. Quadrapole-time-of-flight tandem mass spectrometry was performed on a QSTAR Elite (Applied Biosystems).

4′-(Benzyloxy)-4-methoxy-3′-methyl-2-nitrobiphenyl (4). Under vacuum reduced pressure, PEG 4600 (29.8 g, 6.48 mmol) was heated at 120 °C for 2 h, then flushed with nitrogen. Compound **3** (5.00 g, 15.4 mmol), 4-bromo-3-nitroanisole (2.39 g, 10.3 mmol), K_2CO_3 (2.84 g, 20.6 mmol), and $Pd(OAc)_2$ (0.12 g, 0.51 mmol) were added in this order, and the mixture was stirred at 120 °C for 48 h. The mixture was cooled and the resulting solid was dissolved in the minimum amount of DCM required for complete dissolution. Ether was slowly added to the mixture until the PEG precipitated out of solution, and the resulting suspension was filtered. This process was repeated twice with the residual PEG. The solvent was removed under reduced pressure and the resulting yellow residue was purified by column chromatography (19:1 hexanes/EtOAc) to give **4** as bright-yellow crystals (1.86 g, 52%); mp 119 °C. ^{1}H NMR (400 MHz, $CDCl_3$): δ 7.46 (d, J = 7.2 Hz, 2H), 7.40 (t, J = 7.2 Hz, 2H), 7.35−7.31 (m, 3H), 7.12 (dd, J_S = 2.8 Hz, J_L = 8.4 Hz, 1H), 7.10 (d, J = 2.0 Hz, 1H), 7.06 (dd, J_S = 2.0 Hz, J_L = 8.4 Hz, 1H), 6.90 (d, J = 8.0 Hz, 1H), 5.11 (s, 2H), 3.89 (s, 3H), 2.30 (s, 3H). ^{13}C NMR (100.6 MHz, $CDCl_3$): δ 158.90, 156.98, 149.87, 137.44, 132.99, 130.57, 129.47, 128.76, 128.60, 128.05, 127.66, 127.36, 126.58, 118.79, 111.53, 109.03, 70.10, 56.11, 16.72.

2-(Benzyloxy)-7-methoxy-1-methyl-9*H*-carbazole (5) and 2-(Benzyloxy)-7-methoxy-3-methyl-9*H*-carbazole (6). Compound **4** (0.50 g, 1.4 mmol) was dissolved in 1,3-dicholorobenzene (1,3-DCB) (2 mL). The solution was purged with nitrogen and kept under a nitrogen atmosphere. TEA triphenylphosphine (0.94 g, 3.6 mmol) was added, and the mixture was refluxed for 48 h. The 1,3-DCB was removed under vacuum reduced pressure, and the residue was taken up in $CHCl_3$, impregnated on silica gel, and purified via column chromatography (3:1 hexanes/EtOAc) to yield both cyclization products **5** and **6** as solids (92%). Compound **5**: R_f = 0.56; yellowish solid (0.22 g); mp 167−168 °C. ^{1}H NMR (400 MHz, $CDCl_3$): δ 7.84 (d, J = 8.4 Hz, 1H), 7.76 (s, 1H), 7.73 (d, J = 8.4 Hz, 1H), 7.50 (d, J = 7.6 Hz, 2H), 7.41 (t, J = 7.6 Hz, 2H), 7.34 (m, 1H), 6.93 (d, J = 2.0 Hz, 1H), 6.91 (d, J = 8.4 Hz, 1H), 6.83 (dd, J_S = 2.0 Hz, J_L = 8.4 Hz, 1H), 5.18 (s, 2H), 3.90 (s, 3H), 2.44 (s, 3H). ^{13}C NMR (100.6 MHz, $CDCl_3$): δ 158.21, 154.40, 141.09, 140.27, 137.76, 128.46, 127.71, 127.29, 120.33, 117.90, 117.67, 116.88, 107.96, 107.69, 106.14, 95.00, 71.33, 55.60, 10.12. Compound **6**: R_f = 0.45; light-tan solid (0.20 g); mp 250−251 °C. ^{1}H NMR (400 MHz, $CDCl_3$): δ 7.80 (d, J = 8.4 Hz, 1H), 7.76 (s, 1H), 7.72 (s, 1H), 7.49 (d, J = 7.2 Hz, 2H), 7.41 (t, J = 7.2 Hz, 2H), 7.33 (m, 1H), 6.89 (s, 1H), 6.87 (d, J = 2.4 Hz, 1H), 6.81 (dd, J_S = 2.4 Hz, J_L = 8.4 Hz, 1H), 5.16 (s, 2H), 3.88 (s, 3H), 2.42 (s, 3H). ^{13}C NMR (100.6 MHz, DMSO-d_6): δ 157.25, 154.53, 140.69, 139.13, 137.56, 128.33, 127.51, 127.11, 120.38, 119.64, 117.34, 116.30, 115.66, 107.05, 94.47, 94.26, 69.20, 55.10, 16.59.

7-Methoxy-1-methyl-9*H*-carbazol-2-ol (7). Compound **5** (0.33 g, 1.0 mmol) was dissolved in MeOH (15 mL). The solution was purged with nitrogen and kept under a nitrogen atmosphere. Ammonium formate (0.65 g, 10.3 mmol) was added with a catalytic amount of 5% Pd/C. After the mixture was stirred for 3 h, the solution was filtered through a plug of Celite, washing with MeOH and EtOAc. The solvent was removed under reduced pressure and the resulting residue taken up in EtOAc (20 mL) and washed with H_2O (3 × 20 mL). The organic layer was dried over $MgSO_4$, and the solvent was removed under reduced pressure. Column chromatography (3:1 hexanes/EtOAc) provided **7** as a yellowish tan solid (0.22 g, 94%); mp 200−202 °C (dec). ^{1}H NMR (400 MHz, DMSO-d_6): δ 10.73 (s, 1H), 9.08 (s, 1H), 7.75 (d, J = 8.4 Hz, 1H), 7.55 (d, J = 8.4 Hz, 1H), 6.89 (d, J = 2.4 Hz, 1H), 6.69 (dd, J_S = 2.4 Hz, J_L = 8.4 Hz, 1H), 6.65 (d, J = 8.4 Hz, 1H), 3.80 (s, 3H), 2.29 (s, 3H). ^{13}C NMR (100.6 MHz, DMSO-d_6): δ 157.05, 152.55, 141.03, 119.47, 117.29, 116.47, 115.10, 113.60, 107.93, 106.61, 104.74, 94.58, 55.19, 10.22.

7-Methoxy-3-methyl-9*H*-carbazol-2-ol (8). The above procedure was followed using compound **6** (0.38 g, 1.2 mmol) as the substrate. The product was purified by column chromatography (3:1 hexanes/EtOAc) to yield **8** as an off-white chalky solid (0.26 g, 97%); mp 238−240 °C (dec). ^{1}H NMR (400 MHz, DMSO-d_6): δ 10.66 (s, 1H), 9.18 (s, 1H), 7.73 (d, J = 8.4 Hz, 1H), 7.60 (s, 1H), 6.84 (d, J = 2.4 Hz, 1H), 6.82 (s, 1H), 6.66 (dd, J_S = 2.4 Hz, J_L = 8.4 Hz, 1H), 3.79 (s, 3H), 2.22 (s, 3H). ^{13}C NMR (100.6 MHz, DMSO-d_6): δ 156.96, 153.45, 140.54, 139.45, 120.27, 119.23, 116.68, 115.79, 114.97, 106.58, 96.02, 94.42, 55.10, 16.40.

7-Methoxy-1-methyl-9*H*-carbazol-2-yl 5-(dimethylamino)naphthalene-1-sulfonate (9). Compound **7** (0.15 g, 0.66 mmol) was dissolved in DCM. Then TEA (0.18 mL, 1.3 mmol) was added, and reaction mixture was stirred for 10 min. Dansyl chloride (0.18 g, 0.66 mmol) was added, and the reaction mixture was stirred for 3 h. Solvent was removed under reduced pressure, the resulting residue impregnated onto silica gel, and the product was purified by column chromatography (3:1 hexanes/EtOAc) to yield **9** as a fluffy yellow solid (0.30 g, 99%); mp 174 °C. ^{1}H NMR (400 MHz, $CDCl_3$): δ 8.62 (d, J = 8.4 Hz, 1H), 8.55 (d, J = 8.4 Hz, 1H), 8.09 (d, J = 7.6 Hz, 1H), 7.95 (s, 1H), 7.75 (d, J = 8.4 Hz, 1H), 7.65 (t, J = 7.6 Hz, 1H), 7.45 (m, 2H), 7.24 (m, 1H), 6.89 (s, 1H), 6.79 (d, J = 8.4 Hz, 1H), 6.33 (d, J = 8.4 Hz, 1H), 3.85 (s, 3H), 2.91 (s, 6H), 2.40 (s, 3H). ^{13}C NMR (100.6 MHz, $CDCl_3$): δ 159.02, 151.82, 145.35, 141.32, 139.32, 132.00, 131.77, 130.91, 130.14, 129.83, 128.93, 123.02,

121.58, 121.08, 119.74, 117.02, 116.81, 115.59, 113.87, 113.57, 108.68, 94.78, 55.60, 45.43, 11.30.

7-Methoxy-3-methyl-9*H*-carbazol-2-yl 5-(dimethylamino)naphthalene-1-sulfonate (10). The above procedure was followed using compound **8** (0.14 g, 0.60 mmol) as the substrate. The product was purified by column chromatography (3:1 hexanes/EtOAc), providing **10** as a yellow solid (0.24 g, 86%); mp 242 °C. ^{1}H NMR (400 MHz, DMSO-d_6): δ 10.96 (s, 1H), 8.66 (d, J = 8.4 Hz, 1H), 8.38 (d, J = 8.4 Hz, 1H), 8.13 (d, J = 7.6 Hz, 1H), 7.89 (d, J = 8.4 Hz, 1H), 7.85 (s, 1H), 7.78 (t, J = 8.0 Hz, 1H), 7.66 (t, J = 8.0 Hz, 1H), 7.37 (d, J = 7.6 Hz, 1H), 6.86 (d, J = 2.4 Hz, 1H), 6.74 (dd, J_S = 2.4 Hz, J_L = 8.4 Hz, 1H), 6.58 (s, 1H), 3.80 (s, 3H), 2.90 (s, 6H), 2.23 (s, 3H). ^{13}C NMR (100.6 MHz, DMSO-d_6): δ 158.52, 151.58, 145.06, 141.71, 137.73, 131.83, 131.26, 130.60, 129.18, 129.06, 128.99, 123.46, 121.46, 120.90, 120.81, 120.72, 118.44, 115.54, 115.07, 107.98, 103.34, 94.29, 55.07, 44.97, 16.39.

Cell Line and Cell Growth Assay. Human prostate cancer cell line PC-3 was procured from the American Type Cell Culture Collection. Cells were grown in IMEM without phenol red (Invitrogen) with 10% fetal bovine serum, 2 mM glutamine, 100 U/mL penicillin G sodium, and 100 μg/mL streptomycin sulfate (Sigma) in the presence of 5% CO_2 at 37 °C. For the cell growth experiment, PC-3 cells were seeded in six-well plates in triplicate with an initial density of 1.5×10^4 cells per well. Twenty-four hours after seeding, the attached cells were treated with vehicle (DMSO) or 1, 5, 15, 30, and 60 μM compound. After another period of 24 h, the cells were washed with 1 × PBS, trypsinized, and resuspended in complete growth medium. Trypan blue (0.4%) was added to the cell suspension, and both live and dead cells were counted using a hemocytometer.

BrdU Labeling. For the BrdU experiment, PC-3 cells were seeded in 96-well plates at a density of 2×10^4 cells/well, treated with 5 μM compound for 24 h and assayed for BrdU using the cell proliferation ELISA BrdU (chemiluminescence) (Roche Diagnostics) kit according to the manufacturer's protocol. Light emission was measured using a microplate luminometer (Harta Instruments, Inc.).

Reverse Transcription Polymerase Chain Reaction (RT-PCR). From PC-3 cells incubated 3 days with either 15 μM compound (**5**−**10**) or 5 μM (mahanine, **9**), RNA was extracted with TRIzol solution (Invitrogen) and genes of interest were amplified using 500 ng of total RNA reverse-transcribed to cDNA using a Superscript II kit (Invitrogen) with random hexamers. Human-specific primers were designed using the Primer Quest program and purchased from Integrated DNA Technologies, Inc. Their sequences and product band sizes are the following: cyclin D1 forward primer 5′-CACACGGACTACAGGGGAGT-3′, cyclin D1 reverse primer 5′-AGGAAGCGGTCCAGGTAGTT-3′ (475 bp), and GAPDH forward primer: 5′-CCA CCCATGGCAAATTCCATGGCA-3′. GAPDH reverse primer: 5′-TCTAGACGGCAG GTCAGGTCCACC-3′ (598 bp). PCRs were initiated at 94 °C for 2 min, followed by 28 cycles of 94 °C for 1 min, 1 min at annealing temperature, 72 °C for 1 min, and final extension at 72 °C for 5 min. The annealing temperature for cyclin D1 and GAPDH was 60 °C. Primers and PCR conditions for RASSF1A were used as previously described.[4] After amplification, PCR products were separated on 1.5% agarose gels and visualized by ethidium bromide fluorescence using the Fuji LAS-1000 Imager. Images were captured and imported to Adobe Photoshop. Band intensities were quantified by using ImageJ software (NIH).

DNA Methyltransferase Activity Assay. PC-3 cells were plated in complete growth media, treated with either 2 μM (mahanine, **9**) or 15 μM (**5**, **6**, **7**, **8**, **10**) compound for 3 days and then were harvested. Nuclear extracts were prepared according to manufacturer's protocol (nuclear extraction kit, Epigentek). DNMT activity was measured using an EpiQuik DNA methyltransferase activity assay kit (Epigentek). Results were expressed as percent DNMT activity compared to the DMSO control as 100%.

Multiphoton Laser Imaging. After incubation of slides with a fibronectin/cortactin solution for 30 min, PC-3 cells were plated onto the slides and incubated overnight. The cells were then treated with a 5 μM solution of compound **9** or DMSO control and incubated for 1−6 h before washing with PBS. The slides were fixed with a 4% formaldehyde solution, washed with PBS, then treated with propidium iodide (nuclear localization) and DNMT3a or DNMT3b. The compound was excited at 725 nm with a multiphoton laser and imaged with a 500−550 nm filter.

Animals. Balb/c mice and athymic Balb/c nude mice were purchased from the National Cancer Institute (NCI). Animals were housed 4−6 per cage with microisolater tops and provided food (Furina mice chow) and water ad libitum. The light cycle was regulated automatically (12 h light/dark cycle), and temperature was maintained at 23 ± 1 °C. All animals were allowed to acclimate to this environment for 1 week prior to experimental manipulations. The Georgetown University Animal Care and Use Committee approved all animal studies in accordance with the guidelines adopted by the National Institutes of Health.

Cell Culture for Xenograft. PC-3 cell line (ATCC, Manassas, VA) was cultured in RPMI-1640 with L-glutamine (Mediatech Inc., Herdon, VA) containing 5% fetal bovine serum (FBS), 2.5 mM L-glutamine at 37 °C with 5% CO_2.

Xenograft Study. Male athymic Balb/c nude mice (18−22 g) were injected with 3×10^6 (0.3 mL) human prostate cancer cells (PC-3). The human prostate cancer cells were injected in the subcutaneous tissue of the right axillary region of the mice. One week after the injection, the mice were randomly sorted into two groups with four mice per group. A stock solution of compound **9** was obtained by dissolving 1 mg of compound in 1 μL of DMSO. The stock was added to polyethylene glycol 400 (PEG) (Hampton) and PBS in a 1:1 ratio. The test concentrations were obtained by diluting with PEG/PBS. The tumor-bearing mice received an intraperitoneal injection (ip) with either 10 mg/kg **9** or vehicle control once every other day for 28 days. At the same time, the tumor size of each mouse was measured by caliper and calculated by the formula length × width × height/2.

Statistical Analyses. Cell data were derived from at least three independent experiments, and animal data were derived from the xenograft study described above. Statistical analyses were conducted using Prism 4 GraphPad software, referencing Li and Yuan[21] for animal evaluation methods. Values are presented as the mean ± SEM.

Acknowledgment. We thank the Lombardi shared resources for technical support and the Georgetown Drug Discovery Program and Lombardi Comprehensive Cancer Center for financial assistance. We also thank Dr. Samir Bhattacharya and Dr. Bikas C. Pal of the Indian Institute of Chemical Biology, Kolkata, India, for providing us with purified mahanine. A patent application has been filed by Georgetown University on the behalf of the inventors that are listed as authors in this article.

Supporting Information Available: NCI data for compound **9** and elemental analysis and HRMS data for compounds **5**−**10**. This material is available free of charge via the Internet at http://pubs.acs.org.

References

(1) Donninger, H.; Vos, M. D.; Clark, G. J. The RASSF1A tumor suppressor. *J. Cell Sci.* **2007**, *120*, 3163–3172.
(2) van der Weyden, L.; Adams, D. J. The Ras-association domain family (RASSF) members and their role in human tumourigenesis. *Biochim. Biophys. Acta* **2007**, *1776*, 58–85.
(3) Dallol, A.; Agathanggelou, A.; Tommasi, S.; Pfeifer, G. P.; Maher, E. R.; Latif, F. Involvement of the *RASSF1A* tumor suppressor gene in controlling cell migration. *Cancer Res.* **2005**, *65*, 7653–7659.

(4) Rong, R.; Jin, W.; Zhang, J.; Sheikh, M. S.; Huang, Y. Tumor suppressor RASSF1A is a microtubule-binding protein that stabilizes microtubules and induces G2/M arrest. *Oncogene* **2004**, *23*, 8216–8230.
(5) Shivakumar, L.; Minna, J.; Sakamaki, T.; Pestell, R.; White, M. A. The RASSF1A tumor suppressor blocks cell cycle progression and inhibits cyclin D1 accumulation. *Mol. Cell. Biol.* **2002**, *22*, 4309–4318.
(6) Vos, M. D.; Martinez, A.; Elam, C.; Dallol, A.; Taylor, B. J.; Latif, F.; Clark, G. J. A role for the RASSF1A tumor suppressor in the regulation of tubulin polymerization and genomic stability. *Cancer Res.* **2004**, *64*, 4244–4250.
(7) Li, L.-C.; Okino, S. T.; Dahiya, R. DNA methylation in prostate cancer. *Biochim. Biophys. Acta* **2004**, *1704*, 87–102.
(8) Liu, L.; Yoon, J.-H.; Dammann, R.; Pfeifer, G. P. Frequent hypermethylation of the *RASSF1A* gene in prostate cancer. *Oncogene* **2002**, *21*, 6835–6840.
(9) Kuzmin, I.; Gillespie, J. W.; Protopopov, A.; Geil, L.; Dreijerink, K.; Yang, Y.; Vocke, C. D.; Duh, F.-M.; Zabarovsky, E.; Minna, J. D.; Rhim, J. S.; Emmert-Buck, M. R.; Linchan, W. M.; Lerman, M. I. The *RASSF1A* tumor suppressor gene is inactivated in prostate tumors and suppresses growth of prostate carcinoma cells. *Cancer Res.* **2002**, *62*, 3498–3502.
(10) Jagadeesh, S.; Sinha, S.; Pal, B. C.; Bhattacharya, S.; Banerjee, P. P. Mahanine reverses an epigenetically silenced tumor suppressor gene *RASSF1A* in human prostate cancer cells. *Biochem. Biophys. Res. Commun.* **2007**, *362*, 212–217.
(11) Beaulieu, N.; Morin, S.; Chute, I. C.; Robert, M.-F.; Nguyen, H.; MacLeod, A. R. An essential role for DNA methyltransferase DNMT3b in cancer cell survival. *J. Biol. Chem.* **2002**, *277*, 28176–28181.
(12) Brueckner, B.; Boy, R. G.; Siedlecki, P.; Musch, T.; Kliem, H. C.; Zielenkiewicz, P.; Suhai, S.; Wiessler, M.; Lyko, F. Epigenetic reactivation of tumor suppressor genes by a novel small-molecule inhibitor of human DNA methyltransferases. *Cancer Res.* **2005**, *65*, 6305–6311.
(13) Wang, L.; Zhang, Y.; Liu, L.; Wang, Y. Palladium-catalyzed homocoupling and cross-coupling reactions of aryl halides in poly(ethylene glycol). *J. Org. Chem.* **2006**, *71*, 1284–1287.
(14) Freeman, A. W.; Urvoy, M.; Criswell, M. E. Triphenylphosphine-mediated reductive cyclization of 2-nitrobiphenyls: a practical and convenient synthesis of carbazoles. *J. Org. Chem.* **2005**, *70*, 5014–5019.
(15) Sinha, S.; Pal, B. C.; Jagadeesh, S.; Banerjee, P. P.; Bandyopadhaya, A.; Bhattacharya, S. Mahanine inhibits growth and induces apoptosis in prostate cancer cells through the deactivation of Akt and activation of caspases. *Prostate* **2006**, *66*, 1257–1265.
(16) Chen, Y.; Martinez, L. A.; LaCava, M.; Coghlan, L.; Conti, C. J. Increased cell growth and tumorigenicity in human prostate LNCaP cells by overexpression to cyclin D. *Oncogene* **1998**, *16*, 1913.
(17) Musgrove, E. A.; Lee, C. S. L.; Buckley, M. F.; Sutherland, R. L. Cyclin D1 induction in breast cancer cells shortens G1 and is sufficient for cells arrested in G1 to complete the cell cycle. *Proc. Natl. Acad. Sci. U.S.A.* **1994**, *91*, 8022–8026.
(18) Kim, G.-D.; Ni, J.; Kelesoglu, N.; Roberts, R. J.; Pradhan, S. Co-operation and communication between the human maintenance and de novo DNA (cytosine-5) methyltransferases. *EMBO J.* **2002**, *21*, 4183–4195.
(19) Majumder, S.; Ghoshal, K.; Datta, J.; Bai, S.; Dong, X.; Quan, N.; Plass, C.; Jacob, S. T. Role of de novo DNA methyltransferases and methyl CpG-binding proteins in gene silencing in a rat hepatoma. *J. Biol. Chem.* **2002**, *277*, 16048–16058.
(20) Organization for Economic Co-Operation and Development. Acute Oral Toxicity (AOT) Up-and-Down-Procedure. http://www.epa.gov/oppfead1/harmonization/.
(21) Li, L. N.; Yuan, S. J. Anti-Tumor Drugs: In Vivo Standards. In *Methodology of New Drug Research in Pharmacology*, 1st ed.; Lu, Q. J., Ed.; Chemical Industry Press: Beijing, 2007; pp 245−247.
(22) Lyko, F.; Brown, R. DNA methyltransferase inhibitors and the development of epigenetic cancer therapies. *J. Natl. Cancer Inst.* **2005**, *97*, 1498–1506.
(23) Pray, L. At the flick of a switch: epigenetic drugs. *Chem. Biol.* **2008**, *15*, 640–641.